THE JOURNAL OF PHYSICAL CHEMISTRY B

Article

pubs.acs.org/JPCB

Cosolvent Effects on Solute−Solvent Hydrogen-Bond Dynamics: Ultrafast 2D IR Investigations

Somnath M. Kashid,[†,‡] Geun Young Jin,[§,‡] Sayan Bagchi,[*,†] and Yung Sam Kim[*,§]

[†]Physical and Materials Chemistry Division—CSIR, National Chemical Laboratory, Dr. Homi Bhabha Road, Pashan, Pune 411008, India

[§]Department of Chemistry, Ulsan National Institute of Science and Technology (UNIST), 50 UNIST-gil, Ulsan 44919, Korea

Supporting Information

ABSTRACT: Cosolvents strongly influence the solute−solvent interactions of biomolecules in aqueous environments and have profound effects on the stability and activity of several proteins and enzymes. Experimental studies have previously reported on the hydrogen-bond dynamics of water molecules in the presence of a cosolvent, but understanding the effects from a solute's perspective could provide greater insight into protein stability. Because carbonyl groups are abundant in biomolecules, the current study used 2D IR spectroscopy and molecular dynamics simulations to compare the hydrogen-bond dynamics of the solute's carbonyl group in aqueous solution, with and without the presence of DMSO as a cosolvent. 2D IR spectroscopy was used to quantitatively estimate the time scales of the hydrogen-bond dynamics of the carbonyl group in neat water and 1:1 DMSO/water solution. The 2D IR results show spectral signatures of a chemical exchange process: The presence of the cosolvent was found to lower the hydrogen-bond exchange rate by a factor of 5. The measured exchange rates were 7.50×10^{11} and 1.48×10^{11} s^{-1} in neat water and 1:1 DMSO/water, respectively. Molecular dynamics simulations predict a significantly shorter carbonyl hydrogen-bond lifetime in neat water than in 1:1 DMSO/water and provide molecular insights into the exchange mechanism. The binding of the cosolvent to the solute was found to be accompanied by the release of hydrogen-bonded water molecules to the bulk. The widely different hydrogen-bond lifetimes and exchange rates with and without DMSO indicate a significant change in the ultrafast hydrogen-bond dynamics in the presence of a cosolvent, which, in turn, might play an important role in the stability and activity of biomolecules.

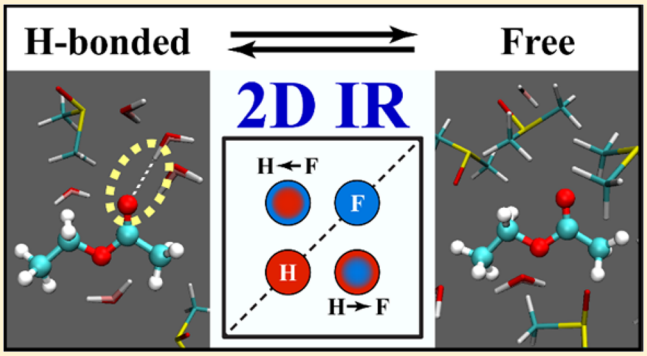

1. INTRODUCTION

The effects of cosolvents on biological systems in aqueous solutions have gained wide attention in recent times. Addition of a cosolvent to an aqueous protein solution changes the properties of the biological molecule, such as protein stability, protein solubility, and protein self-assembly. The choice of the cosolvent to perturb the conformational equilibrium of proteins in aqueous buffer can either prevent or favor protein denaturation.[1−4] Theoretical studies have been performed to understand the effect of cosolvents on protein stability.[5−10] Solute−cosolvent interactions are often viewed as an exchange process where the binding of the cosolvent is accompanied by the release of water molecules to the bulk.[6,11,12] Cosolvents also have profound effects on the activity of several enzymes.[13,14] Cosolvents act as cryoprotectants and are used for preserving stem cells, organs, and sperms in aqueous solutions. Understanding the basic mechanisms of such behavior can help in engineering desired properties of proteins and enzymes.

Because of its infinite solubility in water at room temperature, dimethyl sulfoxide (DMSO) is a widely used cosolvent in aqueous solutions. DMSO, a relatively polar molecule that is capable of accepting hydrogen bonds, has the ability to disrupt the hydrogen-bonded structure of water and associate itself with proteins, nucleic acids, carbohydrates, and ionic substances. As a cosolvent, DMSO has many important implications in the fields of chemistry, biology, and pharmacology.[15−21] DMSO has commonly been used as a cosolvent to solubilize small organic molecules and thus has an application as a drug carrier along cell membranes.[22] Depending on the concentration of DMSO in solution, protein stability and enzymatic activity can be altered.[23−25] Several experimental methods, including vibrational spectroscopy, neutron scattering, and dielectric spectroscopy, have been used to study the structural properties of DMSO/water solutions.[26−30] The effects of hydrogen bonding on DMSO/water solutions were recently studied using X-ray absorption, emission, and scattering experiments.[31] Theoretical and computational studies have also been performed to elucidate the structure of DMSO/

Received: September 4, 2015
Revised: November 11, 2015
Published: November 11, 2015

DOI: 10.1021/acs.jpcb.5b08643
J. Phys. Chem. B 2015, 119, 15334−15343

water mixtures.[17,32] Although several scientific studies have focused on the structural changes and interactions in DMSO/water solutions with varying DMSO concentrations, a consistent picture regarding the effects of DMSO as a cosolvent on water dynamics has yet to be formulated. Whereas NMR and dielectric relaxation experiments predict significant slowing of the rotational motions of water in the presence of DMSO, other experiments involving neutron scattering and Raman-induced Kerr-effect spectroscopy have reported faster rotational times as compared with bulk water.[30,33−37] A very recent study by Fayer and co-workers using polarization-selective pump−probe experiments and two-dimensional infrared (2D IR) spectroscopy focused on the ultrafast dynamics of dilute HOD in DMSO/water solutions.[38] Their experimental results describe the structural dynamics of water on multiple time scales, ranging from the very fast dynamics of local hydrogen-bond fluctuations to the slower dynamics of complete structural randomization.

Although the water hydrogen-bond dynamics in DMSO/water solutions have been studied, most of the studies focused on understanding the dynamics from the solvent's perspective. The effects of DMSO as a cosolvent on a solute molecule in the presence of water have yet to be explored. Understanding the changes in dynamics from the solute's perspective will provide a deeper insight into changes in protein stability upon addition of a cosolvent. In this article, we report the carbonyl−water hydrogen-bond dynamics as sensed by the ester carbonyl (C═O) group in ethyl acetate (EtOAc), both in the presence and in the absence of the cosolvent DMSO. On the basis of IR/NMR correlations it was recently suggested that the ester carbonyl in EtOAc, exists in two different environments in DMSO/water solutions and the two populations exchange on time scales much faster than NMR time resolution.[39]

Two-dimensional infrared spectroscopy has proved to be a very powerful experimental technique for investigating ultrafast structural fluctuations and exchange dynamics in small molecules and proteins in the solution phase.[40−61] In this study, we used 2D IR spectroscopy to observe the ultrafast dynamics of the ester C═O stretching mode of EtOAc in aqueous solution and in 1:1 (v/v) DMSO/water solution. The 2D IR results indicate two different environments of the ester C═O group even in the absence of DMSO, undergoing chemical exchange on a ∼1.3-ps time scale. This time scale quantitatively matches the reported time scale of hydrogen-bond making and breaking in bulk water. Chemical exchange on ultrafast time scales has also been reported for small-molecule esters such as EtOAc and methyl acetate (MeOAc) in neat solvents.[48,49] Upon addition of DMSO, our 2D IR results confirm the earlier prediction of chemical exchange,[39] but the exchange time scale is ∼6.8 ps, which is much slower than that in bulk water. This study also reports molecular dynamics (MD) simulations performed on EtOAc in neat water and in 1:1 DMSO/water solution. Carbonyl hydrogen-bond analysis of the MD trajectories predicts chemical exchange in both solvation environments; the hydrogen-bond making and breaking process in the presence of the cosolvent was found to be significantly slower than that in neat water. The ratio of the carbonyl hydrogen-bond lifetime of EtOAc in neat water and in 1:1 DMSO/water, as predicted from MD simulations, is comparable to the ratio of experimentally obtained exchange time scales, with and without the presence of DMSO. A detailed analysis of the MD snapshots provides a molecular-level picture of the exchange mechanism in the presence of the cosolvent. Because carbonyl groups are abundant in the protein backbone and side chains, our current study will help to interpret results for complex biomolecular systems. The results described herein will also provide new insights into the solvation dynamics of small molecules in the presence of a cosolvent.

2. EXPERIMENTAL METHODS

Samples. Solutions of 40 mM EtOAc in D_2O and 1:1 (v/v) DMSO/water were used for the linear infrared (IR) absorption and 2D IR experiments. EtOAc, D_2O, and DMSO were purchased from Sigma-Aldrich and used without further purification. All reported spectra were collected at room temperature (22 °C).

Linear IR Spectroscopy. Fourier-transform infrared (FTIR) absorption spectra were recorded on a Varian 670-IR spectrometer with 0.25 cm^{-1} resolution. For each sample, ∼8 μL of the sample solution was loaded in a demountable sample cell consisting of two CaF_2 windows separated by a Teflon spacer of 25-μm thickness.

2D IR Spectroscopy. In a typical 2D IR experiment, three ultrashort IR pulses having controlled polarization and tuned to the carbonyl stretching frequency of EtOAc (∼1720 cm^{-1}) were focused at the sample. The 2D IR experimental schemes and data-processing procedures were reported previously.[62] The IR pulses used for 2D IR experiments (60 fs in duration, almost transform limited; see Figure S1, Supporting Information) were generated by a homemade optical parametric amplifier (OPA) that was pumped by a Ti:sapphire regenerative amplifier (Spitfire Pro-35F-1KXP). The three successive IR pulses with wave vectors $\mathbf{k}_1$, $\mathbf{k}_2$, and $\mathbf{k}_3$ were applied to the sample to induce the subsequent emission of the vibrational echo. The vibrational echo in the phase-matching direction ($\mathbf{k}_s = -\mathbf{k}_1 + \mathbf{k}_2 + \mathbf{k}_3$) is detected, with frequency and phase resolution, by combining it with a local oscillator (LO) pulse. The LO pulse precedes the echo signal by an interval of ∼1 ps. The combined pulses are focused at the focal plane of a monochromator (TRIAX-190) and detected by a 64-element mercury cadmium telluride (MCT) IR array detector (InfraRed Associates), enabling the signal to be measured as a function of detection time, t. Each 2D IR vibrational echo data point is a function of three variables: the emitted vibrational echo frequency (ω_t), the variable time interval between the first and second pulses (τ), and the variable time separation between the second and third pulses (T). The focal length of the monochromator was 190 mm, and the groove density of the grating used in the monochromator for the 2D IR experiments was 150 lines/mm. The time interval τ was scanned from −3 to 3 ps in 2-fs steps, where negative and positive values represent nonrephasing and rephasing schemes, respectively. All 2D IR spectra shown here were collected with parallel polarization and represent the real part of the absorptive (correlation) spectra. The 2D spectra are displayed as the double Fourier transforms of the (τ, t) data set with frequency arguments (ω_τ, ω_t).

Numerical Simulation of the Linear and 2D IR Spectra. Linear IR and 2D IR spectra were numerically simulated incorporating exchange processes during the two coherence periods (τ and t) as well as the waiting time (T). The numerical simulations were based on the previous works by Kim and Hochstrasser.[41,43] Static and dynamic parameters were obtained by iterative least-squares fitting of the simulated spectra with the experimental FTIR and 2D IR spectra. Details of the

DOI: 10.1021/acs.jpcb.5b08643
J. Phys. Chem. B 2015, 119, 15334−15343

numerical simulation methodology are presented in section 4 of the Supporting Information.

3. SIMULATION METHODS

Molecular dynamics simulation of EtOAc in neat water and in 1:1 DMSO/water solution were performed with the GROMACS simulation package[63,64] (version 4.6.5) and the general AMBER force field (GAFF)[65] following a recent study[66] that benchmarked the reliability of GAFF and optimized potentials for liquid simulations/all-atom (OPLS/AA) for modeling a wide range of organic liquids including DMSO and EtOAc. The force field parameters of the organic liquids were obtained from virtualchemistry.org.[67] Water was modeled using the TIP4P-Ew model.[68] Prior to each simulation, an energy minimization using a steepest-descent algorithm was performed, followed by equilibration in the *NVT* ensemble at 300 K for 100 ps using the velocity rescale thermostat[69] and equilibration in the *NPT* ensemble at 300 K and 1 bar (using a Parrinello−Rahman barostat[70]) for 1 ns. The coordinates were recorded for a 5-ns MD production run every 4 fs and used for the analysis of hydrogen-bond dynamics. We adopted a geometric definition for defining a hydrogen bond between the carbonyl oxygen of EtOAc and a water molecule. The O—H bond of a water molecule was considered to be hydrogen-bonded if the O(donor)—O(acceptor) distance was less than 3.5 Å and the H—O(donor)—O(acceptor) angle was less than 30°.

4. RESULTS AND DISCUSSION

Linear IR Spectra. The background-subtracted FTIR spectra for the C═O stretch of EtOAc in three environments, namely, water (water refers to D_2O), DMSO, and 1:1 DMSO/water solution, are shown in Figure 1. In water, a broad asymmetric curve for the ester C═O vibration, having its peak maximum at 1703.5 cm^{-1}, is observed, whereas a single sharp peak appears at 1732.8 cm^{-1} in DMSO. In 1:1 DMSO/water solution, two peaks of comparable magnitudes are observed, separated by ∼20 cm^{-1}. The IR absorption spectra of the C═O stretch in EtOAc dissolved in either neat water or 1:1 DMSO/water can be approximately fitted with two Voigt profiles. However, in the aprotic solvent DMSO, the low-frequency peak completely disappears, leaving only the high-frequency peak, which can be fitted reasonably well using a single Voigt profile. As mentioned in an earlier work,[39] the peak position of the higher-frequency peak in the presence of the cosolvent, DMSO, is closer to that in neat DMSO (non-hydrogen-bonded), whereas the lower-frequency peak corresponds to the population where C═O is hydrogen-bonded to solvent water molecules, leading to a red shift in the absorption maximum. However, a single peak in the ^{13}C NMR spectrum for the carbonyl carbon of EtOAc in 1:1 DMSO/water solution[39] suggests the existence of ultrafast hydrogen-bond exchange dynamics on time scales that cannot be detected by NMR spectroscopy and inspired us to apply the 2D IR spectroscopic approach to understand the ultrafast dynamics in the presence of the cosolvent DMSO.

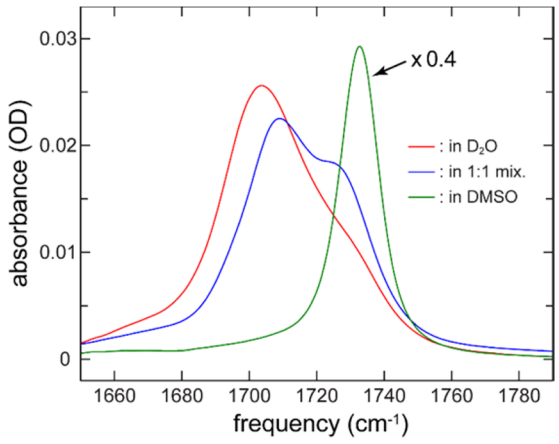

Figure 1. FTIR spectra of EtOAc in (red) D_2O, (blue) 1:1 DMSO/water mixture, and (green) DMSO. The concentration of the solutions was 40 mM, and the path length was 25 μm. The spectrum in DMSO was multiplied by a factor of 0.4.

2D IR Spectra. The ester C═O hydrogen-bond exchange dynamics of EtOAc in both 1:1 DMSO/water solution and neat water were studied separately using 2D IR spectroscopy to understand the effects of DMSO as a cosolvent on the carbonyl hydrogen bond in aqueous solution. The experimental absorption and 2D IR spectra of EtOAc in 1:1 DMSO/water at various waiting times (T = 0, 1, 2, 3, and 4 ps) are shown at the left column in Figure 2. In the 2D IR spectra, the red and blue peaks represent the $\nu = 0 \rightarrow 1$ and $\nu = 1 \rightarrow 2$ transitions, respectively. As seen in the linear IR spectra of EtOAc in 1:1 DMSO/water (Figure 1), two major transitions are clearly observed in the 2D IR spectra at ∼1708 and ∼1730 cm^{-1} along the ω_τ axis. In a 2D IR experiment, the first laser pulse simultaneously labels the initial structures of both free (F) and hydrogen-bonded (H) carbonyl groups with the initial frequencies ω_τ. At T = 0, none of the labeled species has changed their structures, so the final frequencies ω_t are the same as the initial frequencies, leading to two pairs of diagonal peaks that are elongated along the diagonal, one pair for hydrogen-bonded C═O at lower frequencies and the other pair for free C═O groups observed at higher frequencies. At longer waiting times, because of the inherent solvent fluctuations, hydrogen-bond making and breaking between the carbonyl group and water lead to the exchange of carbonyl groups from the free to the hydrogen-bonded population and vice versa. This is manifested in the waiting-time-dependent 2D IR spectra as cross-peaks appearing between the two pairs of diagonal peaks, and the relative magnitude of the cross-peaks with respect to the diagonal peaks increases with increasing values of T. For example, the cross-peak at $(\omega_\tau, \omega_t) \approx$ (1708, 1730 cm^{-1}), which is not present in the 2D IR spectrum at T = 0, is clearly discernible at T = 4 ps, and the spectral region of interest becomes rectangular in shape.[41,46] The cross-peaks observed with increasing values of T are distinctive spectral features of fast chemical exchange dynamics between two different structural configurations. In this case, hydrogen-bond making and breaking between the EtOAc carbonyl and the water molecules are responsible for the appearance of the cross-peaks between the two involved transitions at ∼1708 and ∼1730 cm^{-1}, arising from hydrogen-bonded and free C═O groups, respectively. To determine the kinetic rates of the hydrogen-bond exchange process, the experimentally obtained 2D IR spectra were fitted to the 2D IR spectra, numerically simulated with a Kubo-Anderson two-state exchange model.[71] The relative magnitudes of the cross-peaks with respect to the diagonal peaks are frequently used to obtain the kinetic parameters of the chemical exchange process, but in this particular case, because of the small frequency separation

DOI: 10.1021/acs.jpcb.5b08643
J. Phys. Chem. B 2015, 119, 15334−15343

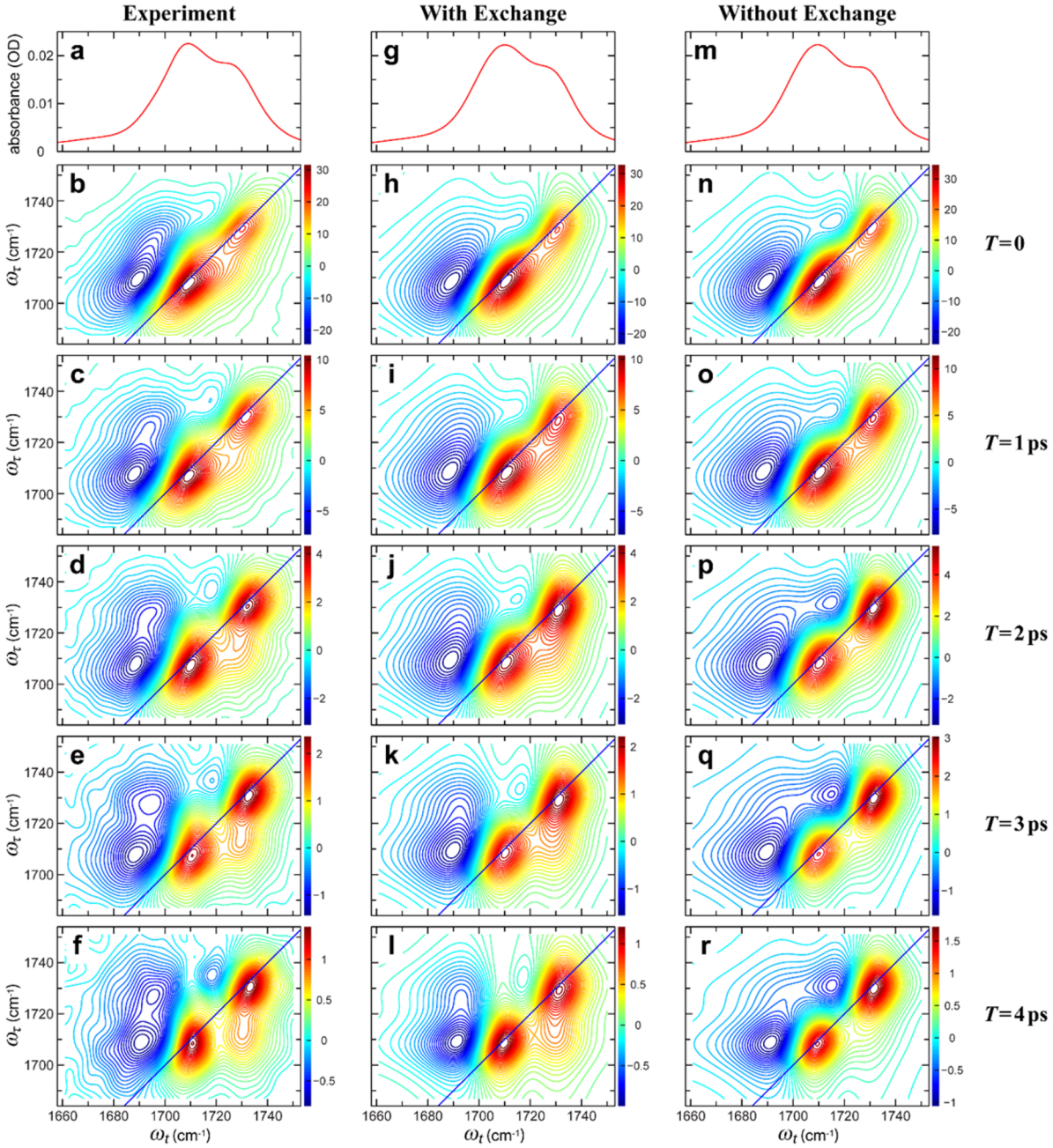

Figure 2. Experimental (left column) and simulated (middle and right columns) linear and 2D IR spectra of EtOAc in a 1:1 DMSO/water mixture. Left column: Experimental (a) linear IR spectrum and (b–f) 2D IR spectra at T = 0, 1, 2, 3, and 4 ps from the top. Middle column: Simulated (g) linear and (h–l) 2D IR spectra at T = 0, 1, 2, 3, and 4 ps (from top to bottom) in the presence of exchange. Right column: Simulated (m) linear and (n–r) 2D IR spectra at T = 0, 1, 2, 3, and 4 ps (from top to bottom) in the absence of exchange.

between the two C═O populations, the overlap between the diagonal and cross-peaks makes the estimation of the magnitudes of the individual peaks extremely difficult. An approach of least-squares fitting of the numerically simulated 2D IR spectrum with the experimental spectrum in the spectral region of interest was used to accurately estimate the kinetic rates of the chemical exchange process. The simulation protocols based on the earlier works by Kim and Hochstrasser[41,43] incorporated the fast-exchange effect during the τ and t coherence periods for both the $\nu = 0 \rightarrow 1$ and $\nu = 1 \rightarrow 2$ transitions. The simulated spectra including exchange parameters are presented in the middle column of Figure 2. The measured exchange rates at the ν = 0 potential surface were 4.76×10^{10} and 1.004×10^{11} s^{-1} for the forward (from H to F, k_{HF}) and backward (from F to H, k_{FH}) exchange processes, respectively. The fact that the rate of formation of hydrogen bond and the rate of dissociation are similar indicates that the system is in equilibrium, with comparable populations of the two states and two off-diagonal cross-peaks growing together. The off-diagonal cross-peak [$(\omega_\tau, \omega_t) \approx$ (1730, 1708 cm^{-1})] arising from the formation of a carbonyl hydrogen bond is indiscernible in either the experimental or the simulated 2D IR spectra, as it overlaps with the more intense negative peak observed from the $\nu = 1 \rightarrow 2$ transition. Assuming that the sum of the exchange rates at the ν = 1 and ν = 2 free-energy surfaces was the same as that at the ν = 0 free-energy surface, the

DOI: 10.1021/acs.jpcb.5b08643
J. Phys. Chem. B 2015, 119, 15334–15343

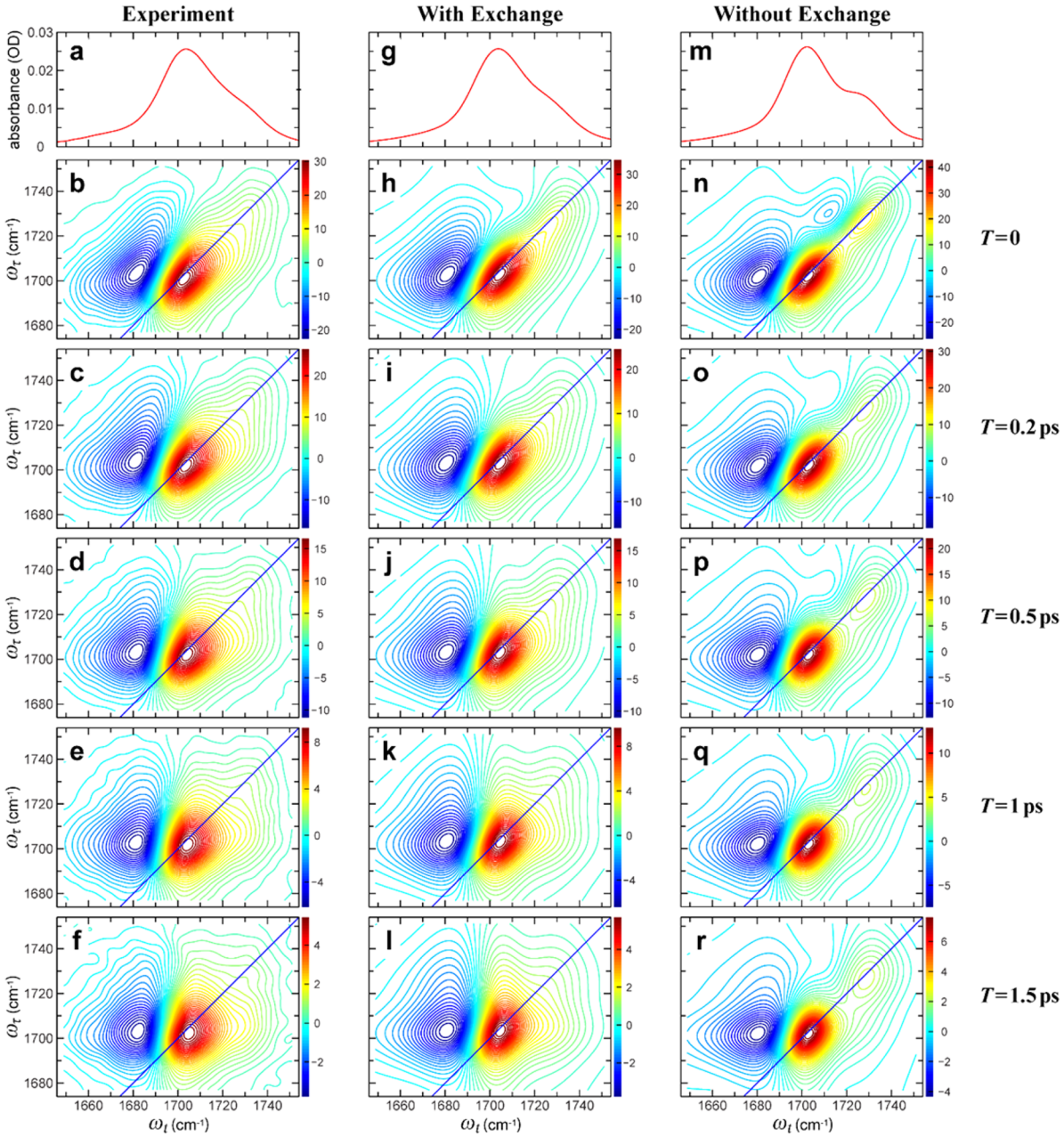

Figure 3. Experimental (left column) and simulated (middle and right columns) linear and 2D IR spectra of EtOAc in D_2O. Left column: Experimental (a) linear IR spectrum and (b–f) 2D IR spectra at T = 0, 0.2, 0.5, 1, and 1.5 ps (from top to bottom). Middle column: Simulated (g) linear and (h–l) 2D IR spectra at T = 0, 0.2, 0.5, 1, and 1.5 ps (from top to bottom) in the presence of exchange. Right column: Simulated (m) linear and (n–r) 2D IR spectra at T = 0, 0.2, 0.5, 1, and 1.5 ps (from top to bottom) in the absence of exchange.

forward and backward rates were estimated to be 4.43×10^{10} and 1.037×10^{11} s^{-1}, respectively, at the $\nu = 1$ surface and 4.04×10^{10} and 1.076×10^{11} s^{-1}, respectively, at the $\nu = 2$ surface. To include intramode spectral diffusion in our simulation, the inhomogeneous line width was varied from 7.82 cm^{-1} at T = 0 to 4.00 cm^{-1} at T = 4 ps for the low-frequency transition (H) and was fixed for the high-frequency transition (F) except at T = 0. All of the parameters used for the numerical simulations are listed in Table S1 of the Supporting Information. To demonstrate the effects of exchange on the spectra, the linear absorption and 2D IR spectra free of exchange were simulated and are presented in the right column of Figure 2. To generate the linear absorption and 2D IR spectra in the absence of exchange, the exchange rates were set to zero, leaving all other simulation parameters unchanged. Even a qualitative comparison of the experimental and simulated spectra reveals that inclusion of chemical exchange processes in the simulations captures most of the distinctive spectral features, including the cross-peaks that appear in the experimental 2D IR spectra with increasing value of T, whereas the cross-peaks are missing in the simulated 2D IR spectra in the absence of exchange. The effect of exchange on the linear IR spectra will be discussed later.

For EtOAc in neat water, experimental linear and 2D IR spectra are presented in the left column of Figure 3, where the 2D IR spectra were obtained at different values of T (T = 0, 0.2, 0.5, 1, and 1.5 ps). The same two-state exchange model as used for EtOAc in 1:1 DMSO/water was used in estimating the exchange rates. Simulated linear and 2D IR spectra in the

DOI: 10.1021/acs.jpcb.5b08643
J. Phys. Chem. B 2015, 119, 15334–15343

presence and absence of exchange are shown in the middle and right columns, respectively, of Figure 3. The measured exchange rates at the $\nu = 0$ potential surface were 2.21×10^{11} and 5.29×10^{11} s^{-1} for the forward (from H to F) and backward (from F to H) exchange processes, respectively. All of the parameters used for the numerical simulations of EtOAc in neat water are listed in Table S2 of the Supporting Information.

The kinetic rate of hydrogen-bond making and breaking in neat water is estimated to be ~5 times higher than that in 1:1 DMSO/water. The higher exchange rate in water suggests that the fluctuations of the water molecules around a C═O group are significantly slowed in the presence of a cosolvent such as DMSO. As the C═O group is surrounded by only water molecules in the neat aqueous environment, the breaking of a hydrogen bond between the C═O group and any water molecule will be followed by the making of another hydrogen bond by the C═O group and another water molecule. In 1:1 DMSO/water solution, the significant decrease in the estimated hydrogen-bond kinetics illustrates a possible change in the solvation environment of the acetate carbonyl. However, experimental results alone cannot provide a molecular-level understanding to explain the change in kinetic rates. Atomistic MD simulations, as discussed later, provide a detailed mechanistic view of the exchange process in the presence of DMSO.

Exchange Effect on Linear IR Spectra. As seen in Figures 2 and 3, the exchange effect was reflected in the 2D IR spectra through the time evolution of the cross-peaks. 2D IR spectroscopy spreads the spectral information in two dimensions, thereby disentangling the overlapping spectral features in a linear absorption spectrum. However, as all the information is available in a linear IR absorption spectrum, the effect of chemical exchange must also appear on the same. This effect will be prominent in the linear absorption spectrum only if the overlap between the two exchanging populations is large. To visualize the effect of exchange on the linear IR absorption spectra of EtOAc in 1:1 DMSO/water and neat water, the experimental and simulated linear absorption spectra shown at the top of Figures 2 and 3 are presented separately at the top of panels a and b, respectively, of Figure 4. For the sample in neat water, the linear absorption spectrum obtained from numerical simulation that includes chemical exchange is a better fit to the experimental spectrum (Figure 4b). This is further confirmed by plotting the difference spectrum between the simulated spectrum (with and without exchange) and the experimental spectrum. However, for EtOAC in 1:1 DMSO/water, inclusion of chemical exchange produces a marginally better fit. In the difference spectra presented at the bottom of Figure 4b (in neat water), the red curve representing the difference between the exchange-included simulated spectrum and the experimental spectrum shows smaller residuals compared to that between the exchange-excluded simulation spectrum and the experimental spectrum (blue curve). For Figure 4a (for 1:1 DMSO/water), not much difference can be observed between the residuals of the numerical simulation with and without chemical exchange. For the case of EtOAc in 1:1 DMSO/water, the total exchange rate of 1.48×10^{11} s^{-1} causes a small effect on the linear IR spectrum; however, deduction of exchange dynamics and its time scale based only on the linear absorption spectrum is not feasible because the line shape of the linear IR spectrum is also dependent on many other factors. For EtOAc in water, the total exchange rate of 7.50×10^{11} s^{-1} causes a greater effect on the linear spectrum. The higher exchange rate in neat water as

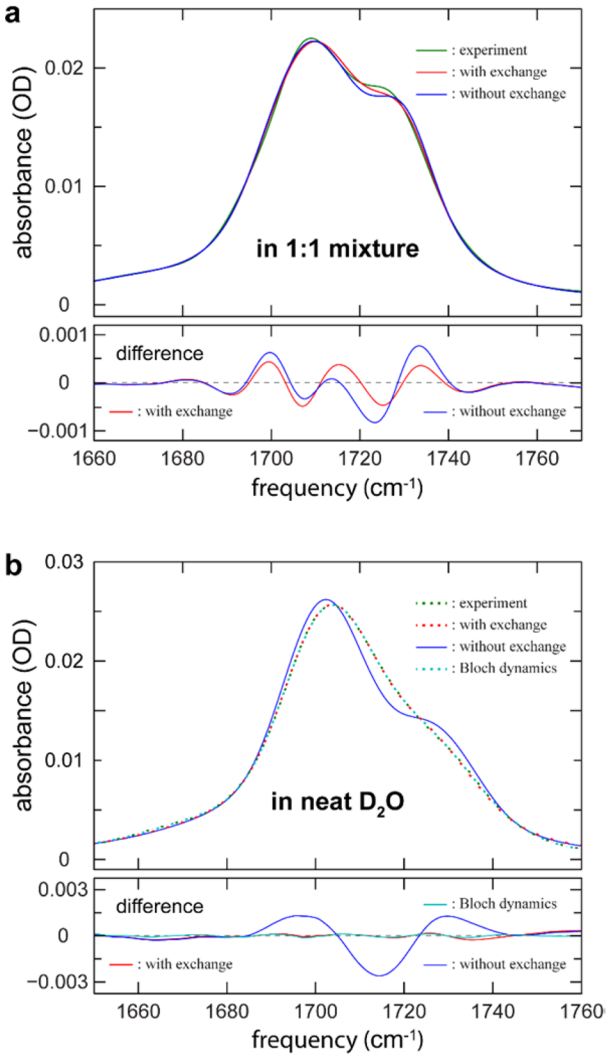

Figure 4. Experimental and simulated linear IR spectra and their differences for EtOAc in (a) a 1:1 mixture of D_2O and DMSO and (b) neat D_2O. Top: Experimental and simulated linear IR spectra. The green, red, and blue curves represent the experimental linear IR spectrum, the simulated linear spectrum including chemical exchange, and the simulated linear spectrum excluding chemical exchange, respectively. The cyan curve in panel b represents the simulated spectrum obtained by applying Bloch dynamics. Bottom: Differences between the experimental and simulated (in the presence of exchange, in the absence of exchange, and in the case of Bloch dynamics) spectra. The red and blue curves represent the differences in the presence of exchange and in the absence of exchange, respectively. The cyan curve in panel b indicates the difference in the case of Bloch dynamics.

compared with 1:1 DMSO/water results in a more visible change in the simulated linear IR spectrum when the exchange process is incorporated in the simulation protocol. However, even in neat water, it is not straightforward to deduce such fast exchange dynamics based only on the linear IR spectrum. For instance, as shown at the top of Figure 4b (cyan curve), we can fit the experimental linear absorption spectrum in neat water reasonably well with simple Voigt profiles without any perception of the exchange processes between the states (Bloch dynamics fitting). This method of curve fitting neglects any effect of coherence transfer, induced by exchange processes, on an IR spectrum. The curve obtained by applying Bloch dynamics is different from that obtained in the absence of

DOI: 10.1021/acs.jpcb.5b08643
J. Phys. Chem. B 2015, 119, 15334−15343

Table 1. Kinetic Rates and Hydrogen-Bond Lifetimes

	forward rate[a] (k_{HF}, s^{-1})			carbonyl H-bond lifetime ratio[b]	
	from 2D IR spectroscopy	from MD simulation	exchange time-scale ratio $(k_{total})_{water}/(k_{total})_{1:1\ mixture}$[b,c] from 2D IR spectroscopy	from 2D IR spectroscopy	from MD simulation
neat water	2.21×10^{11}	2.34×10^{11}	5.1	4.6	4.0
1:1 DMSO/water	4.76×10^{10}	5.90×10^{10}			

[a]As the lifetimes were obtained from the inverse of the forward (hydrogen-bond-breaking) rates, only the forward rates from 2D IR and MD simulations are reported. [b]Ratios rounded to one decimal place. [c]k_{total} is defined as $k_{total} = k_{HF} + k_{FH}$.

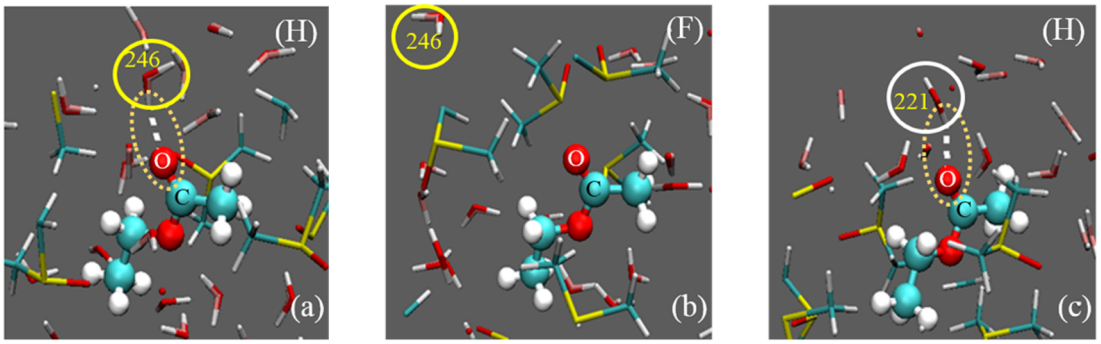

Figure 5. Representative snapshots from MD simulations showing the typical process of breaking and re-forming a carbonyl hydrogen bond: (a) hydrogen-bonded state where water no. 246 (yellow circle) forms a hydrogen bond with the carbonyl of EtOAc, (b) free state where water no. 246 (yellow circle) is released to the bulk, and (c) hydrogen-bonded state where water no. 221 (white circle) forms a hydrogen bond with the solute carbonyl group. H and F indicate hydrogen-bonded and free carbonyl, respectively.

exchange. To generate the curve in the absence of exchange, we used an exchange-incorporated model, but the exchange rates were set to zero. (See section 4a and Table S3 in the Supporting Information.) The results obtained using Bloch dynamics would cause a non-negligible error in interpreting the structural distribution and dynamics of the system (see Figure S2 of the Supporting Information for comparison of the two differently simulated spectra). 2D IR spectroscopy, however, by spreading the spectral information in two dimensions and capturing time-dependent dynamics, unveils spectral features not visible in a linear IR spectrum and thus provides a more sophisticated and accurate approach in investigating fast exchange dynamics occurring on the picosecond time scale. In general, for a carbonyl group dissolved in water, hydrogen-bond exchange between networks of water molecules around the carbonyl group is expected to cause coherence transfer between the states, which, in turn, would significantly affect the shape of its linear IR spectrum. For an accurate interpretation of linear IR spectra of molecular systems undergoing fast exchange as in the case of EtOAc in water, it is necessary to include coherence transfer caused by the exchange process.

Molecular Dynamics Simulation. MD simulations of EtOAc in neat water and in 1:1 DMSO/water solution were carried out to directly compare the effects of the cosolvent (DMSO) on the carbonyl hydrogen-bond dynamics in aqueous solution. Several simulation results were previously reported on the hydrogen-bond distribution and dynamics of the DMSO/water solutions.[17,18,72] The simulations reported here focus on the change in C═O···water hydrogen-bond dynamics with and without the presence of DMSO. The rate constants for the breaking and re-formation of the carbonyl hydrogen bond with water molecules were derived from the g_hbond module of GROMACS simulation package, using the Luzar and Chandler description of hydrogen-bond kinetics.[73] A binary function $h(t)$ was defined such that it is unity when the carbonyl is hydrogen-bonded to any water molecule and zero otherwise. As derived from a chemical dynamics analysis, the autocorrelation function $C_h(t)$ of $h(t)$, also known as the "intermittent HB correlation function",[74] provides the kinetic rates of the hydrogen-bond breaking and making processes.[75] The forward rates obtained from the MD simulations are 2.34×10^{11} and 5.90×10^{10} s^{-1} in neat water and in 1:1 DMSO/water, respectively. The hydrogen-bond lifetime in this scheme is given by the inverse of the forward rate constant estimated from MD simulations.[75] The carbonyl hydrogen-bond lifetime in 1:1 DMSO/water was found to be 4 times longer than that in neat water. All of the kinetic rates and hydrogen-bonding lifetimes are listed in Table 1.

Comparison of Experimental and Simulation Results. Because of the intrinsic fluctuations of the solvent molecules around the solute carbonyl, the average lifetime of the carbonyl hydrogen bond is correlated with the exchange rate of hydrogen-bond breaking and re-formation. A significantly faster exchange time scale is obtained in neat water (1.3 ps) as compared to 1:1 DMSO/water (6.8 ps) from the 2D IR experiments. The forward rate corresponding to the hydrogen-bond breaking process, as obtained from fitting the numerically simulated 2D IR spectrum to the experimental counterpart, was estimated to be lower in the presence of the cosolvent. This result suggests that a hydrogen bond formed between the C═O group and a nearby water molecule will remain intact for a longer period of time in 1:1 DMSO/water. The average hydrogen-bond lifetimes estimated from MD simulations in similar solvation environments are longer in 1:1 DMSO/water than in neat water. 2D IR experiments predict the exchange rate to decrease by a factor of ~5 in the presence of cosolvent, which is in good agreement with the lifetimes being longer by a factor of 4, as obtained from MD simulations. Considering only the inverse forward rates, as estimated from the 2D IR results, the average hydrogen-bond lifetime is 4.6 times shorter in neat water than in the presence of DMSO. Overall, both the experimental and simulation results predict a slower exchange

DOI: 10.1021/acs.jpcb.5b08643
J. Phys. Chem. B 2015, 119, 15334−15343

process in 1:1 DMSO/water than in neat water. The estimated rates from MD simulations and 2D IR experiments, as listed in Table 1, show excellent agreement in neat water. In 1:1 DMSO/water, the estimated rate from the MD simulations is within a factor of 1.25 of our experimental results.

The good agreement of the 2D IR and MD simulation results allowed us to achieve a molecular-level understanding of the hydrogen-bond exchange process of the solute's carbonyl group in the presence of a cosolvent from the MD snapshots. A detailed analysis showed that the H state corresponds to the configuration in which the solute carbonyl is hydrogen-bonded to water and the DMSO molecules are near the alkyl groups, farther from the carbonyl. The intrinsic solvent fluctuations lead to the F state, where DMSO molecules are positioned near the carbonyl and thereby occlude any water molecule from forming a hydrogen bond with the carbonyl oxygen. Interchange between the H and F states was observed throughout the simulation run. The MD snapshots representative of the molecular mechanism of the exchange phenomenon in the presence of DMSO are shown in Figure 5.

It was previously postulated that the solute−water interactions in the presence of a cosolvent can be viewed as an exchange process where the binding of the cosolvent to the solute is accompanied by the release of water molecules to the bulk.[6,11,12] Our 2D IR experimental results directly verify the existence of such an exchange process, and the MD simulation results validate the molecular mechanism suggested above. The water molecule (water no. 246 in the simulation box) that has been hydrogen-bonded to the carbonyl group (highlighted by a yellow circle in Figure 5a) is released to the bulk (highlighted by a yellow circle in Figure 5b) once the DMSO molecules come closer to the carbonyl group. Another water molecule (water no. 221, highlighted by a white circle in Figure 5c), which was not within 5 Å of the solute molecule in the previous hydrogen-bonded configuration, forms a hydrogen bond with the carbonyl grop. The molecular picture obtained from the simulations suggests that there is a constant exchange between the water molecules in the vicinity of the solute and the bulk. DMSO molecules temporarily occlude the exchanging water molecules from forming hydrogen bonds with the carbonyl group and thereby make the hydrogen-bond breaking and reformation processes slower.

The slowing of the hydrogen-bond dynamics of the solute's carbonyl group in the presence of DMSO illustrates the importance of ultrafast dynamics toward biological processes, as a change in the concentration of DMSO in aqueous solution has been reported to alter both the protein stability and enzymatic activity.[23−25] A detailed study probing the ultrafast dynamics as a function of DMSO concentration in DMSO/water solution would likely provide further insight into the concentration dependence of cosolvents toward protein stability. Our experimental results probing the dynamics from the solute's perspective elucidate that addition of DMSO as a cosolvent leads to the change in hydrogen-bond dynamics, which, in turn, is related with the protein function and stability.

5. CONCLUDING REMARKS

We have investigated how DMSO as a cosolvent affects the dynamics of hydrogen-bonding interactions between the C═O group of EtOAc and water by quantitatively estimating the hydrogen-bond exchange rate with and without DMSO in aqueous solution. Ultrafast 2D IR vibrational echo experiments were used to estimate the dissociation and formation rates of carbonyl hydrogen bonds with surrounding water molecules. The estimated exchange rates are 7.50×10^{11} and 1.48×10^{11} s^{-1} in water and 1:1 DMSO/water solution, respectively. MD simulations, performed in similar solvation environments, complement the 2D IR experimental results, as the hydrogen-bond lifetime is estimated to be significantly longer for EtOAc in 1:1 DMSO/water. Structural snapshots from the MD simulations provide a detailed mechanistic picture of the chemical exchange process. The decreasing rate of hydrogen-bond exchange in the presence of DMSO in aqueous solution suggests that the DMSO is capable of perturbing the C═O hydrogen-bond interactions. This work provides a fundamental understanding of how cosolvents affect the solvation dynamics as sensed by the solute molecule and can offer valuable insight into control and leverage solvent dynamics to engineer desired properties of biomolecules. Moreover, these results lead to a direct verification that solute−solvent interactions in the presence of a cosolvent is an exchange process where some of the solvents molecules are released to the bulk upon the binding of the cosolvent with the solute molecules. Our results provide an initial insight about the role of cosolvent toward protein denaturing mechanism where the carbonyl hydrogen-bonding stabilizes the protein secondary structure. Finally, our results provide an experimental way to investigate the mechanistic role of cosolvents in reactions involving a hydrogen-bonded vibrational probe using the 2D IR spectroscopic technique.

■ ASSOCIATED CONTENT

Ⓢ Supporting Information

The Supporting Information is available free of charge on the ACS Publications website at DOI: 10.1021/acs.jpcb.5b08643.

IR pulse spectrum and characteristics, detailed comparison of the numerically simulated linear IR absorption spectra, list of parameters used for the numerical simulations of the 2D IR spectra of EtOAc in neat water and in 1:1 DMSO/water, and methodological details of the numerical simulations for generating linear and 2D IR spectra in the presence of exchange (PDF)

■ AUTHOR INFORMATION

Corresponding Authors

*E-mail: s.bagchi@ncl.res.in. Tel.: +91-20-25903048. Fax: +91-20-25902636.

*E-mail: kimys@unist.ac.kr. Tel.: +82-52-217-2530. Fax: +82-52-217-2649.

Author Contributions

‡S.M.K. and G.Y.J. contributed equally to this work.

Notes

The authors declare no competing financial interest.

■ ACKNOWLEDGMENTS

This work was financially supported by CSIR-NCL MLP Grant 028126. S.B. thanks the Department of Science and Technology (DST) for a Ramanujan Fellowship. Y.S.K acknowledges financial support from the National Research Foundation of Korea (Grant 2011-0015061) and the 2010 Research Fund of UNIST. The authors thank Dr. Suman Chakrabarty (CSIR-NCL, Pune, India) for valuable suggestions regarding MD simulations.

DOI: 10.1021/acs.jpcb.5b08643
J. Phys. Chem. B 2015, 119, 15334−15343

REFERENCES

(1) Timasheff, S. N. The Control of Protein Stability and Association by Weak Interactions with Water: How Do Solvents Affect These Processes. *Annu. Rev. Biophys. Biomol. Struct.* **1993**, *22*, 67−97.

(2) Buck, M. Trifluoroethanol and Colleagues: Cosolvents Come of Age. Recent Studies with Peptides and Proteins. *Q. Rev. Biophys.* **1998**, *31*, 297−355.

(3) Ignatova, Z.; Gierasch, L. M. Effects of Osmolytes on Protein Folding and Aggregation in Cells. *Methods Enzymol.* **2007**, *428*, 355−372.

(4) Jain, N. K.; Roy, I. Effect of Trehalose on Protein Structure. *Protein Sci.* **2009**, *18*, 24−36.

(5) Timasheff, S. N. Control of Protein Stability and Reactions by Weakly Interacting Cosolvents: The Simplicity of the Complicated. *Adv. Protein Chem.* **1998**, *51*, 355−432.

(6) Schellman, J. A. Protein Stability in Mixed Solvents: A Balance of Contact Interaction and Excluded Volume. *Biophys. J.* **2003**, *85*, 108−125.

(7) Auton, M.; Bolen, D. W. Application of the Transfer Model to Understand How Naturally Occuring Osmolytes Affect Protein Stability. *Methods Enzymol.* **2007**, *428*, 397−418.

(8) Record, M. T.; Anderson, C. F. Interpretation of Preferential Interaction Coefficients of Nonelectrolytes and of Electrolyte Ions in Terms of a Two-Domain Model. *Biophys. J.* **1995**, *68*, 786−794.

(9) Pierce, V.; Kang, M.; Aburi, M.; Weerasinghe, S.; Smith, P. E. Recent Applications of Kirkwood-Buff Theory to Biological Systems. *Cell Biochem. Biophys.* **2008**, *50*, 1−22.

(10) Shimizu, S. Estimating Hydration Changes upon Biomolecular Reactions from Osmotic Stress, High Pressure, and Preferential Hydration Experiments. *Proc. Natl. Acad. Sci. U. S. A.* **2004**, *101*, 1195−1199.

(11) Schellman, J. A. Selective Binding and Solvent Denaturation. *Biopolymers* **1987**, *26*, 549−559.

(12) Schellman, J. A. The Thermodynamics of Solvent Exchange. *Biopolymers* **1994**, *34*, 1015−1026.

(13) Watanabe, K.; Ueji, S.-i. Dimethyl Sulfoxide as a Co-Solvent Dramatically Enhances the Enantioselectivity in Lipase-Catalysed Resolutions of 2-Phenoxypropionic Acyl Derivatives. *J. Chem. Soc., Perkin Trans. 1* **2001**, 1386−1390.

(14) Yang, Z. W.; Tendian, S. W.; Carson, W. M.; Brouillette, W. J.; Delucas, L. J.; Brouillette, C. G. Dimethyl Sulfoxide at 2.5% (V/V) Alters the Structural Cooperativity and Unfolding Mechanism of Dimeric Bacterial NAD+ Synthetase. *Protein Sci.* **2004**, *13*, 830−841.

(15) Catalan, J.; Diaz, C.; Garcia-Blanco, F. Characterization of Binary Solvent Mixtures of DMSO with Water and Other Cosolvents. *J. Org. Chem.* **2001**, *66*, 5846−5852.

(16) Brink, G.; Falk, M. Effect of Dimethyl Sulfoxide on Structure of Water. *J. Mol. Struct.* **1970**, *5*, 27−30.

(17) Luzar, A.; Chandler, D. Structure and Hydrogen Bond Dynamics of Water−Dimethyl Sulfoxide Mixtures by Computer Simulations. *J. Chem. Phys.* **1993**, *98*, 8160−8173.

(18) Vaisman, II; Berkowitz, M. L. Local Structural Order and Molecular Associations in Water DMSO Mixtures-Moecular Dynamics Study. *J. Am. Chem. Soc.* **1992**, *114*, 7889−7896.

(19) Kaatze, U.; Pottel, R.; Schäfer, M. Dielectric Spectrum of Dimethyl Sulfoxide/Water Mixtures as a Function of Composition. *J. Phys. Chem.* **1989**, *93*, 5623−5627.

(20) Shashkov, S. N.; Kiselev, M. A.; Tioutiounnikov, S. N.; Kiselev, A. M.; Lesieur, P. The Study of DMSO/Water and DPPC/DMSO/Water System by Means of the X-Ray, Neutron Small-Angle Scattering, Calorimetry and IR Spectroscopy. *Phys. B* **1999**, *271*, 184−191.

(21) Szmant, H. H. Physical Properties of Dimethyl Sulfoxide and Its Function in Biological Systems. *Ann. N. Y. Acad. Sci.* **1975**, *243*, 20−23.

(22) Martin, D.; Hauthal, H. G. *Dimethyl Sulfoxide*; Wiley: New York, 1975.

(23) Pace, C. N. Determination and Analysis of Urea and Guanidine Hydrochloride Denaturation Curves. *Methods Enzymol.* **1986**, *131*, 266−80.

(24) Makhatadze, G. I. Thermodynamics of Protein Interactions with Urea and Guanidinium Hydrochloride. *J. Phys. Chem. B* **1999**, *103*, 4781−4785.

(25) Ramírez-Silva, L.; Oria-Hernández, J.; Uribe, S. Proteins in Water−Cosolvent Binary Systems: Function and Structure. In *Encyclopedia of Surface and Colloid Science*, 2nd ed.; Somasundaran, P., Ed.; Taylor and Francis: Boca Raton, FL, 2006; Vol. 7, pp 5299−5313.

(26) Soper, A. K.; Luzar, A. A Neutron Diffraction Study of Dimethyl Sulfoxide−Water Mixtures. *J. Chem. Phys.* **1992**, *97*, 1320−1331.

(27) Soper, A. K.; Luzar, A. Orientation of Water Molecules around Small Polar and Nonpolar Groups in Solution: A Neutron Diffraction and Computer Simulation Study. *J. Phys. Chem.* **1996**, *100*, 1357−1367.

(28) Wulf, A.; Ludwig, R. Structure and Dynamics of Water Confined in Dimethyl Sulfoxide. *ChemPhysChem* **2006**, *7*, 266−272.

(29) Sastry, M. I. S.; Singh, S. Self-Association of Dimethyl Sulfoxide and Its Dipolar Interactions with Water: Raman Spectral Studies. *J. Raman Spectrosc.* **1984**, *15*, 80−85.

(30) Lu, Z.; Manias, E.; Macdonald, D. D.; Lanagan, M. Dielectric Relaxation in Dimethyl Sulfoxide/Water Mixtures Studied by Microwave Dielectric Relaxation Spectroscopy. *J. Phys. Chem. A* **2009**, *113*, 12207−12214.

(31) Engel, N.; Atak, K.; Lange, K. M.; Gotz, M.; Soldatov, M.; Golnak, R.; Suljoti, E.; Rubensson, J.-E.; Aziz, E. F. DMSO-Water Clustering in Solution Observed in Soft X-Ray Spectra. *J. Phys. Chem. Lett.* **2012**, *3*, 3697−3701.

(32) Borin, I. A.; Skaf, M. S. Molecular Association between Water and Dimethyl Sulfoxide in Solution: A Molecular Dynamics Simulation Study. *J. Chem. Phys.* **1999**, *110*, 6412−6420.

(33) Ludwig, R.; Farrar, T. C.; Zeidler, M. D. Temperature Dependence of the Deuteron and Oxygen Quadrupole Coupling Constants of Water in the System Water/Dimethyl Sulfoxide. *J. Phys. Chem.* **1994**, *98*, 6684−6687.

(34) Gordalla, B. C.; Zeidler, M. D. Molecular Dynamics in the System Water-Dimethylsulfoxide: A NMR Relaxation Study. *Mol. Phys.* **1986**, *59*, 817−828.

(35) Gordalla, B. C.; Zeidler, M. D. NMR Proton Relaxation and Chemical Exchange in the System $H^{16}{}_2O/H^{17}{}_2O$-[$^2H_6$]-Dimethylsulfoxide. *Mol. Phys.* **1991**, *74*, 975−984.

(36) Cabral, J. T.; Luzar, A.; Teixeira, J.; Bellissent-Funel, M. C. Single-Particle Dynamics in Dimethyl-Sulfoxide/Water Eutectic Mixture by Neutron Scattering. *J. Chem. Phys.* **2000**, *113*, 8736−8745.

(37) Wiewior, P. P.; Shirota, H.; Castner, E. W. Aqueous Dimethyl Sulfoxide Solutions: Inter- and Intra-Molecular Dynamics. *J. Chem. Phys.* **2002**, *116*, 4643−4654.

(38) Wong, D. B.; Sokolowsky, K. P.; El-Barghouthi, M. I.; Fenn, E. E.; Giammanco, C. H.; Sturlaugson, A. L.; Fayer, M. D. Water Dynamics in Water/DMSO Binary Mixtures. *J. Phys. Chem. B* **2012**, *116*, 5479−5490.

(39) Kashid, S. M.; Bagchi, S. Experimental Determination of the Electrostatic Nature of Carbonyl Hydrogen-Bonding Interactions Using IR-NMR Correlations. *J. Phys. Chem. Lett.* **2014**, *5*, 3211−3215.

(40) Woutersen, S.; Mu, Y.; Stock, G.; Hamm, P. Hydrogen-Bond Lifetime Measured by Time-Resolved 2D-IR Spectroscopy: N-Methylacetamide in Methanol. *Chem. Phys.* **2001**, *266*, 137−147.

(41) Kim, Y. S.; Hochstrasser, R. M. Chemical Exchange 2D IR of Hydrogen-Bond Making and Breaking. *Proc. Natl. Acad. Sci. U. S. A.* **2005**, *102*, 11185−11190.

(42) Zheng, J.; Kwak, K.; Asbury, J.; Chen, X.; Piletic, I. R.; Fayer, M. D. Ultrafast Dynamics of Solute−Solvent Complexation Observed at Thermal Equilibrium in Real Time. *Science* **2005**, *309*, 1338−1343.

(43) Kim, Y. S.; Hochstrasser, R. M. Comparison of Linear and 2D IR Spectra in the Presence of Fast Exchange. *J. Phys. Chem. B* **2006**, *110*, 8531−8534.

(44) Kim, Y. S.; Hochstrasser, R. M. The Two-Dimensional IR Responses of Amide and Carbonyl Modes in Water Cannot Bed Described by Gaussian Frequency Fluctuations. *J. Phys. Chem. B* **2007**, *111*, 9697−9701.

DOI: 10.1021/acs.jpcb.5b08643
J. Phys. Chem. B 2015, 119, 15334−15343

(45) Ishikawa, H.; Kwak, K.; Chung, J. K.; Kim, S.; Fayer, M. D. Direct Observation of Fast Protein Conformational Switching. *Proc. Natl. Acad. Sci. U. S. A.* **2008**, *105*, 8619−8624.
(46) Kim, Y. S.; Hochstrasser, R. M. Applications of 2D IR Spectroscopy to Peptides, Proteins, and Hydrogen-Bond Dynamics. *J. Phys. Chem. B* **2009**, *113*, 8231−8251.
(47) Dunbar, J. A.; Arthur, E. J.; White, A. M.; Kubarych, K. J. Ultrafast 2D-IR and Simulation Investigations of Preferential Solvation and Cosolvent Exchange Dynamics. *J. Phys. Chem. B* **2015**, *119*, 6271−6279.
(48) Candelaresi, M.; Pagliai, M.; Lima, M.; Righini, R. Chemical Equilibrium Probed by Two-Dimensional IR Spectroscopy: Hydrogen Bond Dynamics of Methyl Acetate in Water. *J. Phys. Chem. A* **2009**, *113*, 12783−12790.
(49) Chuntonov, L.; Pazos, I. M.; Ma, J.; Gai, F. Kinetics of Exchange Between Zero-, One-, and Two-Hydrogen-Bonded States of Methyl and Ethyl Acetate in Methanol. *J. Phys. Chem. B* **2015**, *119*, 4512−4520.
(50) Park, S.; Odelius, M.; Gaffney, K. J. Ultrafast Dynamics of Hydrogen Bond Exchange in Aqueous Ionic Solutions. *J. Phys. Chem. B* **2009**, *113*, 7825−7835.
(51) Omta, A. W.; Kropman, M. F.; Woutersen, S.; Bakker, H. J. Negligible Effect of Ions on the Hydrogen-Bond Structure in Liquid Water. *Science* **2003**, *301*, 347−349.
(52) Kropman, M. F.; Bakker, H. J. Dynamics of Water Molecules in Aqueous Solvation Shells. *Science* **2001**, *291*, 2118−2120.
(53) Fecko, C. J.; Eaves, J. D.; Loparo, J. J.; Tokmakoff, A.; Geissler, P. L. Ultrafast Hydrogen-Bond Dynamics in the Infrared Spectroscopy of Water. *Science* **2003**, *301*, 1698−1702.
(54) Eaves, J. D.; Loparo, J. J.; Fecko, C. J.; Roberts, S. T.; Tokmakoff, A.; Geissler, P. L. Hydrogen Bonds in Liquid Water Are Broken Only Fleetingly. *Proc. Natl. Acad. Sci. U. S. A.* **2005**, *102*, 13019−13022.
(55) Gaffney, K. J.; Ji, M.; Odelius, M.; Park, S.; Sun, Z. H-Bond Switching and Ligand Exchange Dynamics in Aqueous Ionic Solution. *Chem. Phys. Lett.* **2011**, *504*, 1−6.
(56) Anna, J. M.; Baiz, C. R.; Ross, M. R.; McCanne, R.; Kubarych, K. J. Ultrafast Equilibrium and Non-Equilibrium Chemical Reaction Dynamics Probed with Multidimensional Infrared Spectroscopy. *Int. Rev. Phys. Chem.* **2012**, *31*, 367−419.
(57) Peng, C. S.; Baiz, C. R.; Tokmakoff, A. Direct Observation of Ground-State Lactam−Lactim Tautomerization Using Temperature-Jump Transient 2D IR Spectroscopy. *Proc. Natl. Acad. Sci. U. S. A.* **2013**, *110*, 9243−9248.
(58) Dunkelberger, E. B.; Woys, A. M.; Zanni, M. T. 2D IR Cross Peaks Reveal Hydrogen−Deuterium Exchange with Single Residue Specificity. *J. Phys. Chem. B* **2013**, *117*, 15297−15305.
(59) Ren, Z.; Ivanova, A. S.; Couchot-Vore, D.; Garrett-Roe, S. Ultrafast Structure and Dynamics in Ionic Liquids: 2D-IR Spectroscopy Probes the Molecular Origin of Viscosity. *J. Phys. Chem. Lett.* **2014**, *5*, 1541−1546.
(60) Thämer, M.; De Marco, L.; Ramasesha, K.; Mandal, A.; Tokmakoff, A. Ultrafast 2D IR Spectroscopy of the Excess Proton in Liquid Water. *Science* **2015**, *350*, 78−82.
(61) Borek, J. A.; Perakis, F.; Hamm, P. Testing For Memory-Free Spectroscopic Coordinates by 3D IR Exchange Spectroscopy. *Proc. Natl. Acad. Sci. U. S. A.* **2014**, *111*, 10462−10467.
(62) Kim, Y. S.; Wang, J.; Hochstrasser, R. M. Two-Dimensional Infrared Spectroscopy of the Alanine Dipeptide in Aqueous Solution. *J. Phys. Chem. B* **2005**, *109*, 7511−7521.
(63) van der Spoel, D.; Lindahl, E.; Hess, B.; Groenhof, G.; Mark, A. E.; Berendsen, H. J. C. GROMACS: Fast, Flexible, and Free. *J. Comput. Chem.* **2005**, *26*, 1701−1718.
(64) Hess, B.; Kutzner, C.; van der Spoel, D.; Lindahl, E. GROMACS 4: Algorithms for Highly Efficient, Load-Balanced, and Scalable Molecular Simulation. *J. Chem. Theory Comput.* **2008**, *4*, 435−447.
(65) Wang, J.; Wolf, R. M.; Caldwell, J. W.; Kollman, P. A.; Case, D. A. Development and Testing of a General Amber Force Field. *J. Comput. Chem.* **2004**, *25*, 1157−1174.
(66) Caleman, C.; van Maaren, P. J.; Hong, M.; Hub, J. S.; Costa, L. T.; van der Spoel, D. Force Field Benchmark of Organic Liquids: Density, Enthalpy of Vaporization, Heat Capacities, Surface Tension, Isothermal Compressibility, Volumetric Expansion Coefficient, and Dielectric Constant. *J. Chem. Theory Comput.* **2012**, *8*, 61−74.
(67) van der Spoel, D.; van Maaren, P. J.; Caleman, C. GROMACS Molecule & Liquid Database. *Bioinformatics* **2012**, *28*, 752−753.
(68) Horn, H. W.; Swope, W. C.; Pitera, J. W.; Madura, J. D.; Dick, T. J.; Hura, G. L.; Head-Gordon, T. Development of an Improved Four-Site Water Model for Biomolecular Simulations: TIP4P-Ew. *J. Chem. Phys.* **2004**, *120*, 9665−9678.
(69) Bussi, G.; Donadio, D.; Parrinello, M. Canonical Sampling through Velocity Rescaling. *J. Chem. Phys.* **2007**, *126*, 014101.
(70) Parrinello, M.; Rahman, A. Polymorphic Transitions in Single Crystals: A New Molecular Dynamics Method. *J. Appl. Phys.* **1981**, *52*, 7182−7190.
(71) Dattagupta, S. *Relaxation Phenomena in Condensed Matter Physics*; Academic Press: Orlando, FL, 1987.
(72) Harpham, M. R.; Levinger, N. E.; Ladanyi, B. M. An Investigation of Water Dynamics in Binary Mixtures of Water and Dimethyl Sulfoxide. *J. Phys. Chem. B* **2008**, *112*, 283−293.
(73) Luzar, A.; Chandler, D. Hydrogen-Bond Kinetics in Liquid Water. *Nature* **1996**, *379*, 55−57.
(74) Luzar, A. Resolving the Hydrogen Bond Dynamics Conundrum. *J. Chem. Phys.* **2000**, *113*, 10663−10675.
(75) van der Spoel, D.; van Maaren, P. J.; Larsson, P.; Timneanu, N. Thermodynamics of Hydrogen Bonding in Hydrophilic and Hydrophobic Media. *J. Phys. Chem. B* **2006**, *110*, 4393−4398.

DOI: 10.1021/acs.jpcb.5b08643
J. Phys. Chem. B 2015, 119, 15334−15343